American Industrial Hygiene Association Journal

ISSN: 0002-8894 (Print) (Online) Journal homepage: https://www.tandfonline.com/loi/aiha20

MEASURING INDOOR AIRFLOW PATTERNS BY USING A SONIC VECTOR ANEMOMETER

M.G. Yost & R.C. Spear

To cite this article: M.G. Yost & R.C. Spear (1992) MEASURING INDOOR AIRFLOW PATTERNS BY USING A SONIC VECTOR ANEMOMETER, American Industrial Hygiene Association Journal, 53:11, 677-680, DOI: 10.1080/15298669291360364

To link to this article: https://doi.org/10.1080/15298669291360364

AIHA JOURNAL Advances in Industrial & Environmental Hygiene

AM. IND. HYG. ASSOC. J. 53(11):677–680 (1992)

4506

MEASURING INDOOR AIRFLOW PATTERNS BY USING A SONIC VECTOR ANEMOMETER*

M.G. Yost†
R.C. Spear

Center for Occupational and Environmental Health, School of Public Health, University of California, Earl Warren Hall, Berkeley, CA 94720

Air-velocity diagrams are used frequently to describe flow patterns into exhaust hoods, but they are applied rarely to problems involving room-scale airflow. This report describes the use of a novel instrument to evaluate airflow patterns associated with dilution ventilation in a test room. Air velocity was measured with a three-dimensional sonic anemometer, which determines velocity by sensing the time of flight of ultrasonic sound pulses. This sonic anemometer can resolve both the magnitude and direction of the vector at low air velocities, making it well suited for large-scale room measurements. Air-velocity measurements were made inside a controlled ventilation test chamber with the anemometer. The time-averaged directional velocity measurements were incorporated into a vector-mapping computer program that provided a visual presentation of the airflow patterns in the chamber. Tests repeated on several different days revealed a reproducible and stable flow pattern. The test results indicate that vector anemometry may be a useful technique for identifying and quantifying room airflow patterns.

Historically, industrial hygienists have appreciated the important role of air movement in the distribution of contaminants in the workplace. Early investigations emphasized source control through ventilation,[1,2] and over the years a large body of work has been devoted to measuring[3] and calculating[4,5] airflow patterns near local exhaust hoods. The most common quantitative description of the flow field around hoods has been air-velocity contour measurements. Although capture efficiency in hoods can be evaluated directly with tracer gases,[6,7] many hygienists continue to rely on velocity readings to indicate the fate of contaminants.

In contrast, velocity measurements have found only limited application in general room ventilation situations, except perhaps to indicate drafts. Room ventilation commonly has been characterized by a well-mixed box model,[8] which quantitatively describes ventilation in terms of the net air exchange or removal rate. This approach has been extended to include mixing factors to account for imperfect mixing[9] and multicompartment models[10] to accommodate buildings with multiple air-exchange coefficients. The air-exchange coefficients in these models can be measured by using tracer gases, but the relationship between these room-averaged parameters and the underlying air motion has received little attention. More recently, the techniques of computational fluid dynamics have been applied to numerically approximate room flow patterns and velocity information from theoretical models.[11]

Air velocity is a vector quantity, characterized by both magnitude and direction in three-dimensional space. Most air-velocity instruments commonly used by hygienists do not provide directional information but instead measure only the velocity magnitude (i.e., speed) along one directional component. Further, most readings are highly time-averaged so that turbulence information is also lost. Velocity vector and turbulence readings could be potentially useful to hygienists, e.g., in locating regions in a room where the capture performance of an exhaust hood might be compromised by room airflow or turbulent dispersion.

In the context of industrial hygiene, vector air-velocity readings have great intuitive appeal as measures of room ventilation because they indicate both the speed and direction of contaminant transport by the air. Compared to a simple scalar measure, a set of directional velocity readings can reveal a great deal of information about the large-scale (e.g., over a few meters) flow pattern in a room. Obtaining directional information requires a vector anemometer, which in the past was practical only in research laboratories because these instruments were costly, were difficult to use and calibrate, and required large computers to gather and analyze the readings. However, advances in electronic and digital technology have lowered the potential cost, size, and complexity of these devices to the point where they may soon be practical for field situations.

EXPERIMENTAL MATERIALS AND METHODS

This research explored the feasibility of using air velocity to describe dilution ventilation in a room. Tests were conducted in a large, indoor chamber with controlled, uniform ventilation. The objective of this work was to obtain velocity vector measurements that would provide qualitative information about the large-scale flow pattern in the test room as well as quantitative information regarding the amount of air movement and turbulence at various points.

*This work was supported by NIOSH Grant No. R03OH01825-02 and Chemical Manufacturers Association Grant No. 610-32-013.

†Author to whom correspondence should be addressed.

Test Chamber

The test chamber illustrated in Figure 1 was designed to deliver uniform dilution ventilation in a horizontal plug flow arrangement. The test chamber working section was 7.9 × 6.7 × 2.7 m, 143 m^3 (26 × 22 × 8.8 ft, 5050 ft^3). Plenums 0.6 m (2 ft) deep completely covered two opposing side walls and distributed the supply and exhaust air. The air entered the inlet plenum at the chamber center line through a 0.4-m (16-in.) round duct located near the ceiling. Exhaust air exited through a perforated duct spanning the floor of the outlet plenum. The plenum walls facing the interior of the chamber were covered with Masonite® panels having 3-mm (⅛-in.) holes on 25-mm (1-in.) centers. The exterior walls of the room were of common wallboard construction with careful sealing of cracks to reduce leakage.

Mechanical ventilation was provided by two 0.6-m (25-in.) industrial blowers in a push-pull configuration. The static pressure was adjusted between the inside and outside of the chamber and maintained at less than 0.1 in. of water. The low-pressure drop across the walls combined with the sealing helped minimize uncontrolled infiltration. Dampers and variable sheaves allow adjustment of the volume flow rate through the chamber, which was set to 5000 ft^3/min. This ventilation rate produced a nominal room time constant of about 1 min.

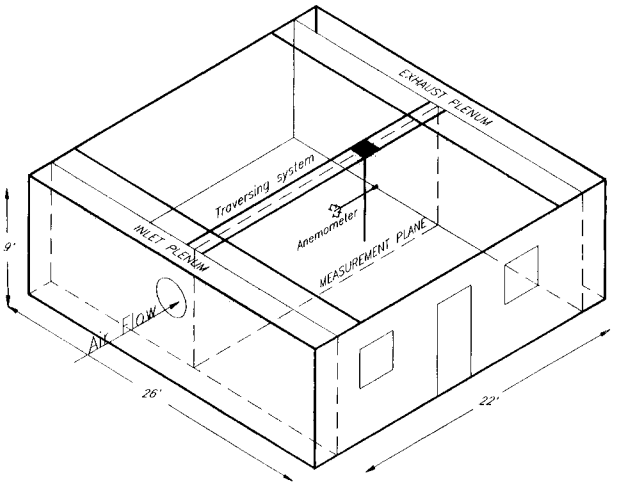

FIGURE 1. Ventilation test chamber. The test chamber is arranged to provide horizontal flow between the inlet and exhaust plenums. The anemometer is shown mounted on the overhead traversing system and positioned in the X-Z measurement plane. Chamber dimensions are rounded to the nearest foot.

Anemometer

Air-velocity measurements were made with a three-component sonic anemometer developed by the Commonwealth Scientific and Industrial Research Organization (CSIRO), an agency of the Australian government. This instrument uses ultrasonic sound pulses to detect the air-velocity components and unambiguously resolve the air-velocity vector; it has a linear response and an absolute calibration that depends only on sensor spacing. It is capable of a wide dynamic range (0.5–2000 cm/sec).[12] The frequency response of this unit was limited to 20 Hz, although theoretically it can achieve a faster response of up to about 300 Hz. Signal-processing capabilities provided digital and analog signals proportional to the velocity components along each axis.

The anemometer operates on the principle that the speed of a sound pressure wave varies with the local air velocity (Figure 2). The system uses 0.9-mm electrostatic condenser transducers, which have a wide, flat frequency response and can either send or receive 100-kHz ultrasonic pulses. Each axis has a pair of digitally switched transducers that alternately emit or listen for a sound pulse. The time needed for a sound pulse to travel in one direction between two transducers in the presence of an air-velocity vector, V, is given by:

$$t_1 = \frac{d}{C \cos \alpha + w} \quad (1)$$

and the travel time in the opposite direction is

$$t_2 = \frac{d}{C \cos \alpha - w} \quad (2)$$

C is the speed of sound, w is the air-velocity component along the axis parallel to the transducers, and α is the angle of the velocity vector compared to the sound path. These travel times are measured directly along each axis defined by a pair of transducers. Three pairs of transducers are arranged at 90° to form an orthogonal, three-dimensional array. The velocity component, w, along a transducer axis is computed by using the inverse of the travel times:

$$\frac{1}{t_2} - \frac{1}{t_1} = \frac{2w}{d} \quad (3)$$

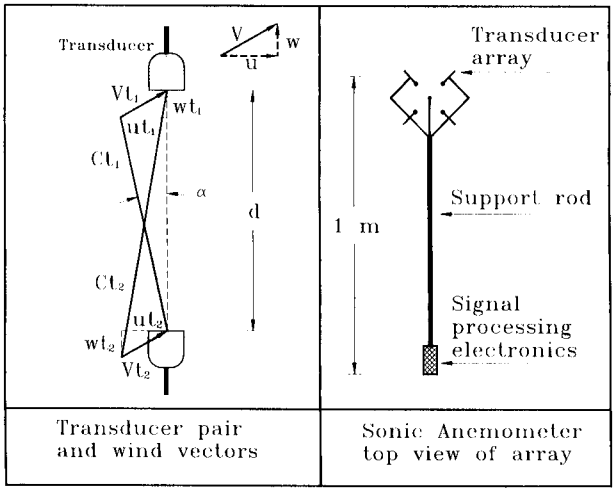

FIGURE 2. Operation of sonic anemometer. A sound pressure wave is speeded up by a tail wind and retarded by a head wind. In this diagram, V is the air-velocity vector, w is the velocity component along the transducer axis, u is the component perpendicular to the transducer axis, α is the angle of deflection, d is the distance between the transducers, and t_1 and t_2 are the travel times for the sound pressure wave in the up and down direction.

Using the inverse of the travel times results in a velocity calibration that depends only on the distance d between the two transducers. Besides giving a linear absolute calibration, the sonic anemometer provides a true line average velocity measurement along the path between the transducers. Prior to the use of digital electronics, the inverse computation technique was not used because it was difficult to implement in analog circuits. The technique has the advantage that it does not depend on the speed of sound and thus does not drift with pressure or temperature.

The digital signals from the anemometer gave real-time readings of the three velocity components and air temperature. These data were entered into a personal computer via an RS-232 serial port and used to determine the mean velocity, eddy velocity, turbulent intensity, turbulent time scale, and kinetic energy flow. The data collection software provided summary statistics as well as continuous recording of the digital data into disk files. CSIRO supplied data collection software written in FORTRAN and machine language, which was subsequently modified for these experiments.

Measurements

A remote-controlled, overhead, two-dimensional traversing system powered by dc motors was used to position the anemometer in a vertical X-Z plane and gather readings in a 5 × 6 grid of points. Each point in a vertical column of five points was scanned for 5 min before moving the anemometer up to the next position. At the end of a column scan sequence, the apparatus moved horizontally to the next of six column locations. In this way, a 30-point grid of velocity readings was collected over a 2.5-hr period. Usually, the entire sequence of measurements was repeated at least once on the same day.

The 5-min sampling interval for the velocity readings was chosen to span at least four room time constants in order to ensure steady-state flow conditions. All people were excluded from the chamber while the 30-point velocity scans were collected to avoid disturbing the flow pattern. Measurements over the 30-point grid were repeated a total of 12 times on 4 different days.

RESULTS AND DISCUSSION

Table I shows the mean velocity data averaged over all experiments. These data are displayed in polar form where the velocity magnitude (U) gives the vector sum of the x, y, and z components. The horizontal angles show the orientation in a positive right-hand coordinate system.

The magnitude k of the fluctuating velocity components at each point was chosen as a summary measure of the total turbulence. This term is closely related to the total turbulent kinetic energy in the flow (= $\frac{1}{2}k^2$) and was calculated by taking the vector sum of the fluctuating velocity components (i.e., component standard deviations) S_x, S_y, and S_z so that $k = \sqrt{Sx^2 + Sy^2 + Sz^2}$.

Table II shows the total turbulence intensity averaged over all experiments, expressed in the table as the total turbulence k divided by the velocity magnitude U. These readings indicate a substantial amount of turbulent energy at all points, with some regions, particularly near the inlet, having very high turbulence levels.

An analysis of variance was used to examine differences between the measurements of a variety of flow parameters repeated at each location on different days. No significant changes were found in the mean vector magnitude, mean velocity components, velocity component fluctuations, or total kinetic energy. The similarity of the data obtained in the same locations at different times and on different days indicated that the flow pattern and turbulence statistics remained stable during the measurements.

Further analysis of the data was conducted with a mapping program entitled VECMAP, written by the authors, which provided a visual display of the velocity readings along with data reduction and interpolation capabilities. A primary application of VECMAP was to generate directional plots of the flow field in a selected plane. These plots consist of a series of line segments with a length proportional to the vector magnitude and a rotation showing the projection of the 3-D vectors onto the viewing plane. Figure 3, a vector map of the velocity measurements, shows the averaged flow field data from Table I.

VECMAP also included provisions for interpolating the flow data between measured grid points and solid boundaries. Vectors at intermediate points are calculated by bilinear interpolation with full three-dimensional rotations and then projected onto the viewing plane.[13] Two boundary conditions were allowed for solid walls: a no-slip condition where all velocity components go to zero at the boundary or a free-slip condition where only the normal velocity component goes to zero. The no-slip condition

TABLE I. Average Velocity Vector Readings in the Measurement Plane

Z^A (ft)	X^B (ft) 3	6	9	12	15	18
7	3.6[C] (109, 40)[D]	8.1 (1, 40)	10.0 (3, 9)	9.8 (9, 1)	10.0 (3, 1)	9.1 (1, 1)
6	13.2 (23, 32)	15.9 (2, 30)	12.1 (2, 9)	9.9 (2, 0)	9.1 (7,0)	9.5 (3, 1)
4.5	28.5 (8, 34)	13.6 (10, 22)	12.5 (2, 0)	9.5 (4, 2)	7.7 (3, 0)	8.5 (2, 1)
3	8.0 (63, 39)	5.4 (32, 25)	8.0 (2, 3)	7.5 (6, 2)	7.7 (1, 8)	7.4 (11, 12)
2	6.4 (144, 37)	3.8 (160, 64)	2.7 (30, 31)	5.1 (9, 9)	5.0 (5, 27)	4.7 (16, 24)

[A]Z = vertical location.

[B]X = horizontal location.

[C]Vector magnitude cm/sec (same for all entries).

[D]Horizontal angle, vertical angle degree (same for all entries).

TABLE II. Turbulence Intensity Measurements (%)

Z^A (ft)	X^B (ft) 3	6	9	12	15	18
7	315[C]	121	84	66	55	49
6	104	75	73	65	58	50
4.5	51	86	76	66	63	48
3	119	181	109	81	62	56
2	104	188	271	116	98	85

[A]Z = vertical location.

[B]X = horizontal location.

[C]Total intensity, % = 100*(k/U).

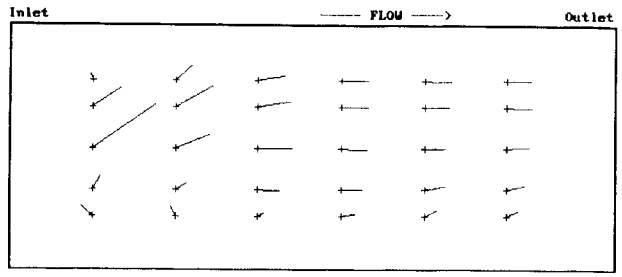

FIGURE 3. Vector diagram of the velocity measurements. The line segments show the magnitude and direction of the average velocity measured at each point.

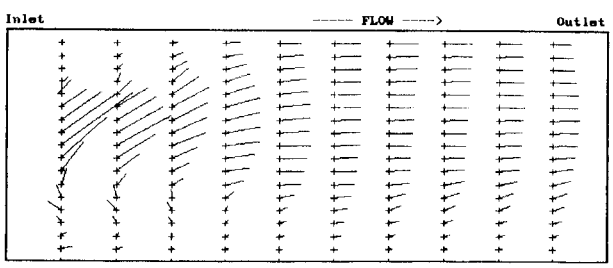

FIGURE 4. Interpolated velocity profiles. The line segments show vertical velocity profiles at 60-cm (2-ft) intervals constructed with the interpolation routine in VECMAP.

assumed a 3-cm boundary layer thickness; the free-slip condition amounted to an infinitesimal boundary layer. In practice, both boundary conditions gave similar results and the free-slip condition was commonly used.

Spot checks of interpolated values were made by comparing them to velocities measured with the anemometer. Generally, there was good agreement between the measured and estimated values, with most readings falling within about ±15% in magnitude and 10° in angle. However, in regions with high turbulence and small mean velocity (>150% total intensity) agreement was poorer with angular deviations up to 70°.

Figure 4 shows an interpolated flow map generated from the averaged flow field data with velocity profiles at intervals of 60 cm (2 ft) along the horizontal axis. The vector diagram clearly shows a strong, high-velocity "jet" tilting upward at the inlet with accompanying highly turbulent recirculation zones above and below. The jet gradually smooths out into a more uniform profile, which appears established within a horizontal distance approximately equal to the vertical height of the room (i.e., 9 ft).

CONCLUSIONS

Overall, the air-velocity vector measurements provided a useful tool for examining the flow patterns in this test chamber. The grid of multiple vector measurements apparently captured both the local flow parameters as well as the larger room-scale directional information. The vector mapping program was an essential aid that provided a visual summary of the velocity measurements and helped clarify the flow pattern. The incorporation of a vector interpolation routine aided in the flow pattern interpretation by allowing the construction of velocity profiles at various selected intervals.

The sonic anemometer performed very well in these low-speed measurements. The instrument was rugged, reliable, and exhibited virtually no drift. The random noise was typically about 0.1 cm/sec, which is not quite as low as expected but still sufficiently low to provide good results. Although this device is presently only a research instrument, it has many desirable features that provide the potential for more widespread use.

The flow pattern in the test chamber was very stable and reproducible over the measurement period. Despite the large inlet plenum, the flow was not homogeneous from inlet to outlet, although there were regions near the outlet with approximately uniform conditions. The jet observed at the inlet corresponded to the location of the air intake to the plenum. This flow pattern was not apparent to people in the room even with the aid of smoke tubes, yet the anemometer identified it easily. Although this research was limited to a well-controlled chamber situation, it demonstrated that a marriage of anemometry and computer mapping can give useful insights into indoor airflows.

REFERENCES

1. **Dalla Valle, J.M. and T. Hatch:** Studies in the Design of Local Exhaust Hoods. *Trans. ASME 54*:31–37 (1932).
2. **Silverman, L.:** Centerline Velocity Characteristics of Narrow Exhaust Slots. *J. Ind. Toxicol. 24*:267–276 (1942).
3. **Flynn, M.R. and M.J. Ellenbecker:** Empirical Validation of Theoretical Velocity Fields into Flanged Circular Hoods. *Am. Ind. Hyg. Assoc. J. 48(4)*:380–389 (1987).
4. **Garrison, R.P. and Y. Wang:** Finite Element Application for Velocity Characteristics of Local Exhaust Inlets. *Am. Ind. Hyg. Assoc. J. 48(12)*:983–988 (1987).
5. **Flynn, M.R. and M.J. Ellenbecker:** The Potential Flow Solution for Air Flow into a Flanged Circular Hood. *Am. Ind. Hyg. Assoc. J. 46(6)*:318–322 (1985).
6. **Kaplan, K.J. and G.W. Knutson:** Laboratory Fume Hoods: A Performance Test. *ASHRAE Trans. 84(1)*:511–521 (1978).
7. **Patterson, R.L., E.L. Schofer, and D.W. Martin:** Laboratory Air Systems—Further Testing. *ASHRAE Trans. 89*:571–596 (1983).
8. **Drivas, P.J., P.G. Simmonds, and F.H. Shair:** Experimental Characterization of Ventilation Systems in Buildings. *Environ. Sci. Technol. 6(7)*:609–614 (1972).
9. **Constance, J.D.:** Mixing Factor is a Guide to Ventilation. *Power 2*:56 (1970).
10. **Sinden, F.W.:** Multi-Chamber Theory of Air Infiltration. *Build. Environ. 13*:21 (1978).
11. **Kern, F.W.:** Integration of Numerical Simulation and Flow Visualization in the Design of Equipment for the Manufacture of Submicron Semiconductor Devices. *J. Environ. Sci. 33(3)*:19–24 (1989).
12. **Coppin, P.A. and K.T. Taylor:** A Three-Component Sonic Anemometer/Thermometer System for General Micrometeorological Research. *Boundary-Layer Meteorol. 27*:27 (1983).
13. **Press, W.H., B.P. Flannery, S.A. Teukolsky, and W.T. Vettering:** *Numerical Recipes, The Art of Scientific Computing*. Cambridge, U.K.: Cambridge Press, 1986.